AIMS Biophysics

AIMS Biophysics, 10(2): 205–219.
DOI: 10.3934/biophy.2023013
Received: 18 January 2023
Revised: 18 April 2023
Accepted: 03 May 2023
Published: 19 May 2023

http://www.aimspress.com/journal/biophysics

Research article

On the dimensionless model of the transcription bubble dynamics

Larisa A. Krasnobaeva[1,2] and Ludmila V. Yakushevich[3,*]

[1] Siberian State Medical University, 634050 Tomsk, Moscow tract 2, Russia
[2] Tomsk State University, 634050 Tomsk, Lenin Avenue 36, Russia
[3] Institute of Cell Biophysics, Russian Academy of Sciences, 142290 Pushchino. Institutskaya str. 3, Moscow region, Russia

* **Correspondence:** Email: kind-@mail.ru; Tel: +74967730252; Fax: +74967330509.

Abstract: The dynamics of transcription bubbles is modeled using a system of nonlinear differential equations, the one-soliton solutions of which (kinks), are interpreted as a mathematical images of transcription bubbles. These equations contain a lot of DNA dynamic parameters, including the moments of inertia of nitrous bases, distances between base pairs, distances from the centers of mass of bases to sugar-phosphate chains, rigidity of the sugar-phosphate backbone, and interactions between bases within pairs. However, estimates of the parameter values are often difficult, and it is not convenient or simple to operate with such multi-parameter systems. One of the ways to reduce the number of the DNA dynamic parameters is to transform the model equations to a dimensionless form. In this work, we construct a dimensionless DNA model and apply it to study transcription bubbles dynamics. We show that transformation to a dimensionless form really leads to a decrease in the number of the model parameters and really simplifies the analysis of model equations and their solutions.

Keywords: transcription bubble; nonlinear DNA model; kinks; McLaughlin-Scott equation; kink trajectories

1. Introduction

It is generally accepted that the transcription bubbles, which are small, locally untwisted regions (or distortions) of the double helix [1–4], are formed at the initial stage of the transcription and then move along the DNA molecule. On the other hand, the DNA molecule is considered by many

researchers as a medium in which nonlinear conformational distortions (or solitary waves) can arise and propagate [5,6]. This amazing property of DNA associates such a purely biological object as DNA with numerous nonlinear, mostly physical systems. Mathematically the movement of the nonlinear distortions are modeled by nonlinear differential equations, in particular, by the nonlinear sine-Gordon equation:

$$\varphi_{\tau\tau} - \varphi_{\xi\xi} + \sin\varphi = 0, \tag{1}$$

having, among others, one-soliton solutions (kinks) [7,8]:

$$\varphi_k(\xi,\tau) = 4\text{arctg}\{\exp[\gamma\cdot(\xi - \upsilon_k\cdot\tau - \xi_0)]\}, \tag{2}$$

where υ_k is the kink velocity; $\gamma = (1-\upsilon_k^2)^{-1/2}$ and ξ_0 is an arbitrary constant.

Beginning with the work of Englander et al. [9], kinks have been actively used to model nonlinear conformational distortions in DNA, of which transcription bubbles are a special case. Currently, to model the dynamics of transcription bubbles, different modifications of the Englander model are used. Usually, they consist of a system of nonlinear differential equations with kink-like solutions. These equations contain many DNA dynamic parameters, such as the moments of inertia of nitrous bases, the distances between base pairs, the distances from the centers of mass of bases to sugar-phosphate chains, the rigidity of the sugar-phosphate backbone and the coefficients characterizing interactions between bases within pairs. Taken together, the equations and their parameters constitute the so-called dimensional model.

To reduce the number of parameters, it is much more convenient and efficient to use a dimensionless analog of a dimensional model. It is believed that the dimensionless analog not only makes it possible to noticeably reduce the number of parameters, but it also significantly simplifies the analysis of equations and methods for finding their solutions. In addition, the results obtained within the dimensionless model are valid not only for DNA, but also for other similar nonlinear media.

In this work, we have constructed a dimensionless analog of the nonlinear differential equations simulating the dynamics of transcription bubbles. We show that carrying out the dimensionless procedure really leads to a decrease in the number of model parameters, as well as to justification of the validity of applying the perturbation theory and the McLaughlin-Scott method [10,11] based on it, which greatly facilitates finding solutions to model equations, their analysis and understanding the nature of the motion of transcription bubbles.

Methods for reducing model equations to a dimensionless form are varied [12–l5]. To simplify calculations, we limited ourselves to the case of homogeneous (synthetic) DNA. In this case, the desired analog can be obtained using a simple transformation from the variables z and t to the new variables ξ and τ:

$$\xi = \sigma z, \tau = \eta t, \tag{3}$$

which is accompanied by additional requirements for the transformation coefficients. We obtained dimensionless model equations, estimated their parameters, found one-soliton solutions (kinks) imitating transcription bubbles and justified the McLaughlin-Scott method, which made it possible to calculate the dimensionless velocity of transcription bubbles and to plot their trajectories in the $\{\xi,\tau\}$ plane.

2. Dimensional DNA model and kink characteristics

Let us consider a homogeneous case when one of the two polynucleotide chains contains only one type of nitrous bases, such as adenines, and the second chain contains only thymines (Figure 1).

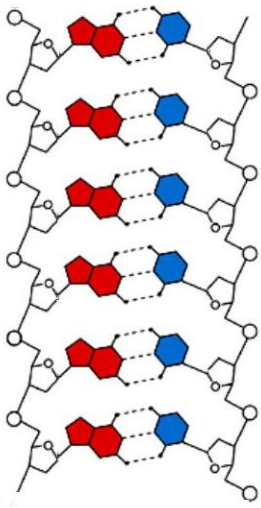

Figure 1. A schematic picture of the double stranded homogeneous DNA. Adenines are shown in red, thymines in blue, sugar-phosphate chains in black-white and hydrogen bonds as dotted lines.

In this case, more general model equations proposed in [16] to describe transcription bubbles dynamics take the following form:

$$\begin{aligned} &I_A \frac{d^2\varphi_{n,A}(t)}{dt^2} - K'_A\left[\varphi_{n+1,A}(t) - 2\varphi_{n,,A}(t) + \varphi_{n-1,A}(t)\right] + \\ &+k_{A-T}R_A(R_A + R_T)\ \sin\varphi_{n,A} - k_{A-T}R_AR_T\sin(\varphi_{n,A} - \varphi_{n,T}) = \\ &= -\beta_A \frac{d\varphi_{n,A}(t)}{dt} + M_0, \end{aligned} \tag{4}$$

$$\begin{aligned} &I_T \frac{d^2\varphi_{n,T}(t)}{dt^2} - K'_T\left[\varphi_{n+1,T}(t) - 2\varphi_{n,T}(t) + \varphi_{n-1,T}(t)\right] + \\ &+k_{A-T}R_T(R_A + R_T)\sin\varphi_{n,T} - k_{A\text{-}T}R_AR_T\sin(\varphi_{n,T} - \varphi_{n,A}) = \\ &= -\beta_T \frac{d\varphi_{n,T}(t)}{dt} + M_0. \end{aligned} \tag{5}$$

Here $\varphi_{n,A}(t)$ and $\varphi_{n,T}(t)$ are the angular displacements of the *n*-th nitrous base in the poly(A) and poly(T) chains, respectively; I_A and I_T are the moments of inertia of the nitrous base in the poly(A) and poly(T) chains, respectively; R_A is the distance from the center of mass of the nitrous base in the poly(A) chain to the sugar-phosphate backbone; R_T is the distance from the center of mass of the nitrous base in the poly(T) chain to the sugar-phosphate backbone; $K'_A = KR_A^2$; $K'_T = KR_T^2$; K is the rigidity of the sugar-phosphate backbone; $\beta_A = \alpha R_A^2$; $\beta_T = \alpha R_T^2$; α is the dissipation coefficient; k_{A-T} is a constant characterizing the interaction between bases within pairs; M_0 is a constant torsion moment.

Equations (4)–(5) take into account only one type of internal DNA motion, namely, angular displacements of the nitrous bases, which is believed to make the main contribution to the opening

base pairs and formation of the transcription babbles. An alternative opinion developed in [17] is that the transverse displacements are more important. The model taking into account only transverse displacements is known as a BP model. In general, a more accurate model imitating the formation dynamics of the transcription bubbles should include both the transverse and angular displacements of the bases, as well as their longitudinal displacements [18].

Despite the limitations of the homogeneous case, equations (4)–(5) contain a fairly large number of dynamic parameters. However, they are only a part of the vast and complex space of parameters used in DNA melting and deformation models [19–21]. Therefore, the question of finding methods to reduce the number of parameters seems to be very relevant.

Restricting themselves to the continuum approximation and taking into account the features of the distribution of interactions within the DNA molecule results in the following: the presence of «weak» hydrogen bonds between nitrous bases inside complementary pairs and «strong» valence interactions along the sugar-phosphate chains; equations (4)–(5) can be reduced (in the first approximation) to two independent equations:

$$I_A\varphi_{A,tt} - K'_A a^2\varphi_{A,zz} + V_A \sin\varphi_A = -\beta_A\varphi_{A,t} + M_0, \tag{6}$$

$$I_T\varphi_{T,tt} - K'_T a^2\varphi_{T,zz} + V_T \sin\varphi_T = -\beta_T\varphi_{T,t} + M_0. \tag{7}$$

Here $V_A = k_{A-T}R_A^2$ and $V_T = k_{A-T}$. The first of these two equations describes the angular displacements of the nitrous bases in the poly(A) chain. The second is the angular displacements of the bases in the complementary chain poly(T). The parameters of equations (6)–(7) are presented in Table 1. The values of the parameters were collected in [22] and then refined in [23].

Table 1. Parameters of the dimensional DNA model.

Homogeneous sequence type	$I\times10^{-44}$ (kg·m^2)	$K'\times10^{-18}$ (N·m)	$V\times10^{-20}$ (J)	$\beta\times10^{-34}$ (J·s)	$M_0\times10^{-22}$ (J)
poly(A)	7.61	2.35	2.09	4.25	3.12
poly(T)	4.86	1.61	1.43	2.91	3.12

2.1. Case $\beta_A \cong 0$, $\beta_T \cong 0$ and $M_0 \cong 0$

In a particular case, when the effects of dissipation and the action of a constant torsion moment are small ($\beta_A \cong 0$, $\beta_T \cong 0$ and $M_0 \cong 0$), equations (6)–(7) take the form of classical sine-Gordon equations, with coefficients depending on the DNA parameters:

$$I_A\varphi_{A,tt} - K'_A a^2\varphi_{A,zz} + V_A \sin\varphi_A = 0, \tag{8}$$

$$I_T\varphi_{T,tt} - K'_T a^2\varphi_{T,zz} + V_T \sin\varphi_T = 0. \tag{9}$$

Let us write Hamiltonians corresponding to equations (8)–(9):

$$H_A = \int \left(I_A \frac{\varphi_{A,t}^2}{2} + K'_A a^2 \frac{\varphi_{A,z}^2}{2} + V_A(1-\cos\varphi_A) \right) \frac{dz}{a}, \tag{10}$$

$$H_T = \int \left(I_T \frac{\varphi_{T,t}^2}{2} + K'_T a^2 \frac{\varphi_{T,z}^2}{2} + V_T(1-\cos\varphi_T) \right) \frac{dz}{a}, \tag{11}$$

and exact one-soliton solutions of equations (8)–(9) – kinks:

$$\varphi_{k,A}(z,t) = 4\text{arctg}\{exp[\,(\gamma_A/d_A)(z - v_{k,A}t - z_{0,A})]\}, \tag{12}$$

$$\varphi_{k,T}(z,t) = 4\text{arctg}\{\exp[\,(\gamma_T/d_T)(z - v_{k,T}t - z_{0,T})]\}. \tag{13}$$

Here, $v_{k,A}$ and $v_{k,T}$ are the kink velocities in the poly(A) and poly(T) chains, respectively; $\gamma_A = (1 - v_{k,A}^2/C_A^2)^{-1/2}$ and $\gamma_T = (1 - v_{k,T}^2/C_T^2)^{-1/2}$ are Lorentz factors; $C_A = (K_A' a^2/I_A)^{1/2}$ and $C_T = (K_T' a^2/I_T)^{1/2}$ are the sound velocities in the chains poly(A) and poly(T), respectively; $d_A = (K_A' a^2/V_A)^{1/2}$ and $d_T = (K_T' a^2/V_T)^{1/2}$ are the kink sizes; $z_{0,A}$ and $z_{0,T}$ are the kink coordinates at the initial moment of time.

The 3D graphs of the two DNA kinks (12)–(13) are presented in Figure 2. They have a canonical kink-like shape, which has been observed in a variety of media, including the mechanical chains of coupled pendulums [24], optical media [25], the chains of Josephson junctions [26–29], crystals [30], superfluid media [27], the Earth's crust [31], ferromagnetic and antiferromagnetic materials [32,33] and biological molecules [34–36].

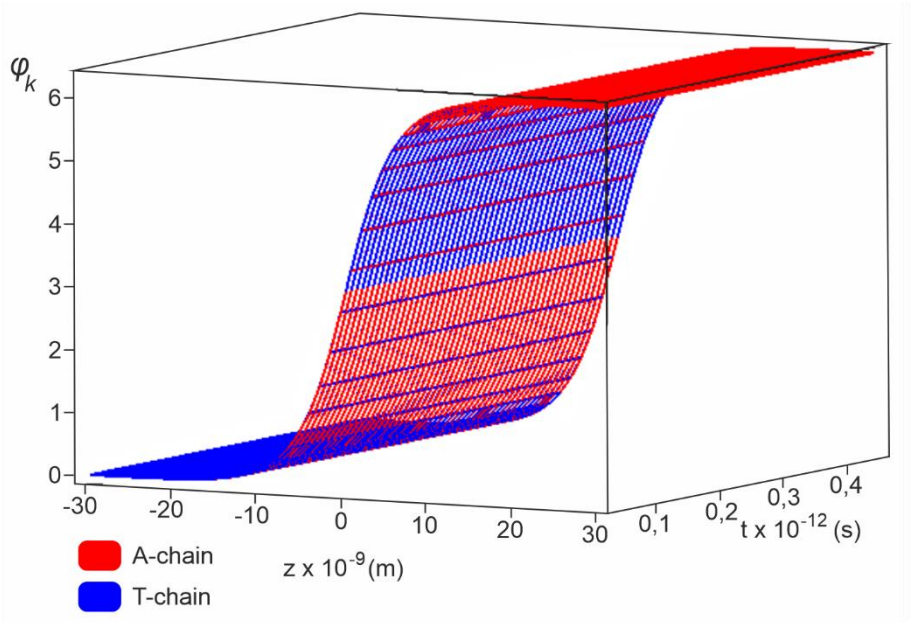

Figure 2. Two DNA kinks moving along the main (red) and complementary (blue) chains. The calculations were carried out with the help of equations (12)–(13) and parameters presented in Table 1.

Substituting equation (12) into equation (10) and equation (13) into equation (11), we find formulas for the kink total energies E_A and E_T:

$$E_A = E_{0,A} \cdot \gamma_A, \tag{14}$$

$$E_T = E_{0,T} \cdot \gamma_T, \tag{15}$$

where E_A and E_T are the the kink rest energies:

$$E_{0,A} = 8\sqrt{K_A' V_A}, \tag{16}$$

$$E_{0,T} = 8\sqrt{K_T' V_T}. \tag{17}$$

In the case of low velocities ($v_{k,A} \ll C_A,\ v_{k,T} \ll C_T$), equations (14) and (15) are transformed into the following form:

$$E_A \cong E_{0,A} + \frac{m_A v_{k,A}^2}{2}, \tag{18}$$

$$E_T \cong E_{0,T} + \frac{m_T v_{k,T}^2}{2}, \tag{19}$$

where $m_A = \frac{E_{0,A}}{2C_A^2}$ and $m_T = \frac{E_{0,T}}{2C_T^2}$ are the masses of kinks propagating along homogeneous poly(A) and poly(T) sequences, respectively. The form of equations (14) and (15) gives reason to consider kinks as quasi-particles having a certain mass, velocity and energy. Using the parameters from Table 1, we calculated the size, rest energy and mass of the kinks activated in the homogeneous poly(A) and poly(T) sequences. The results are presented in Table 2.

Table 2. Physical characteristics of the kinks in the dimensional DNA model.

Homogeneous sequence type	*d* (nm)	$E_0 \times 10^{-18}$ (J)	$m \times 10^{-25}$ (kg)
poly(A)	3.61	1.77	2.48
poly(T)	3.61	1.21	1.58

2.2. Case $\beta_A \neq 0,\ \beta_T \neq 0$ and $M_0 \neq 0$

For the general case, when $\beta_A \neq 0,\ \beta_T \neq 0$ and $M_0 \neq 0,$ exact solutions of equations (6)–(7) have not yet been found. Approximate solutions of these equations, obtained by the method of McLaughlin and Scott [10,11], have a form similar to equations (12)–(13):

$$\varphi_{k,A}(z,t) = 4\mathrm{arctg}\{\exp[(\gamma_A/d_A)(z - v_{k,A}(t)\cdot t - z_{0,A})]\}, \tag{20}$$

$$\varphi_{k,T}(z,t) = 4\mathrm{arctg}\{\exp[(\gamma_T/d_T)(z - v_{k,T}(t)\cdot t - z_{0,T})]\}. \tag{21}$$

However, unlike equations (12)–(13), in equations (20)–(21), the kink velocities $v_{k,A}(t)$ and $v_{k,T}(t)$ are the functions of time, which are determined by the following equations:

$$\frac{dv'_{k,A}(t)}{dt} = -\frac{\beta_A}{I_A} v'_{k,A}(t)(1 - {v'_{k,A}}^2(t)) + \frac{M_0\pi}{4\sqrt{I_A V_A}}(1 - {v'_{k,A}}^2(t))^{3/2}, \tag{22}$$

$$\frac{dv'_{k,T}(t)}{dt} = -\frac{\beta_T}{I_T} v'_{k,T}(t)(1 - {v'_{k,T}}^2(t)) + \frac{M_0\pi}{4\sqrt{I_T V I_T}}(1 - {v'_{k,T}}^2(t))^{3/2}. \tag{23}$$

Here, $\upsilon'_{k,A}(t) = \frac{\upsilon_{k,A}(t)}{c_A}$) and $\upsilon'_{k,T}(t) = \frac{\upsilon_{k,T}(t)}{c_T}$are the relative kink velocities.

Having determined the kink coordinates from the relations $\upsilon_{k,A}(t) = \frac{dz_{k,A}}{dt}$ and $\upsilon_{k,T}(t) = \frac{dz_{k,T}}{dt}$, we have constructed the kinks trajectories on the plane {z, t} by using the method proposed in [37], where, however, only one of the two DNA polynucleotide chains was considered. Here, we extended this method to the model (4) – (5), which took into account two DNA polynucleotide chains.

3. Dimensionless DNA model and kink characteristics

Let us consider the transformation from variables *z* and *t* to new variables ξ and τ according to equation (3). To find the transformation coefficients σ and η, substitute equation (22) into equations (6) and (7), respectively:

$$I_A\eta^2\varphi_{A,\tau\tau} - K_A^{/}a^2\sigma^2\varphi_{A,\xi\xi} + V_A\sin\varphi_A = -\beta_A\eta\varphi_{A,\tau} + M_0, \tag{24}$$

$$I_T\eta^2\varphi_{T,\tau\tau} - K_T^{/}a^2\sigma^2\varphi_{T,\xi\xi} + V_T\sin\varphi_T = -\beta_T\eta\varphi_{T,\tau} + M_0. \tag{25}$$

Next, let us multiply and divide equations (24) and (25) by $\left(I_A\eta^2\right)$:

$$(I_A\eta^2)\left(\varphi_{A,\tau\tau} - \frac{K_Aa^2\sigma^2}{I_A\eta^2}\varphi_{A,\xi\xi} + \frac{V_A}{I_A\eta^2}\sin\varphi_A\right) = (I_A\eta^2)\left(-\frac{\beta_A\eta}{(I_A\eta^2)}\varphi_{A,\tau} + \frac{M_0}{(I_A\eta^2)}\right), \tag{26}$$

$$(I_A\eta^2)\left(\frac{I_T}{I_A}\varphi_{T,\tau\tau} - \left(\frac{K_Aa^2\sigma^2}{I_A\eta^2}\right)\frac{K_T}{K_A}\varphi_{T,\xi\xi} + \left(\frac{V_A}{I_A\eta^2}\right)\frac{V_T}{V_A}\sin\varphi_T\right) = (I_A\eta^2)\left(-\frac{\beta_A\eta}{(I_A\eta^2)}\frac{\beta_T}{\beta_A}\varphi_{T,\tau} + \frac{M_0}{(I_A\eta^2)}\right), \tag{27}$$

and require the fulfillment of two conditions:

$$\frac{K_A^{/}a^2\sigma^2}{I_A\eta^2} = 1, \quad \frac{V_A}{I_A\eta^2} = 1, \tag{28}$$

from which we find the transformation coefficients σ and η:

$$\eta = \sqrt{\frac{V_A}{I_A}}, \quad \sigma = \sqrt{\frac{V_A}{K_1^{/}\alpha^2}}. \tag{29}$$

In the new variables, equations (26) and (27) take the following form:

$$\varphi_{A,\tau\tau} - \varphi_{A,\xi\xi} + \sin\varphi_A + \tilde{\beta}_A\varphi_{A,\tau} - \tilde{M}_{0,A} = 0, \tag{30}$$

$$i_{AT}\varphi_{T,\tau\tau} - k_{AT}\varphi_{T,\xi\xi} + v_{AT}\sin\varphi_T + \tilde{\beta}_T\varphi_{T,\tau} - \tilde{M}_{0,A} = 0, \tag{31}$$

where $\tilde{\beta}_A = \frac{\beta_A}{I_A\eta} = \frac{\beta_A}{\sqrt{I_AV_A}}$, $\tilde{\beta}_T = \frac{\beta_T}{I_A\eta} = \frac{\beta_T}{\sqrt{I_AV_A}}$, $\tilde{M}_{0,A} = \frac{M_0}{I_A\eta^2} = \frac{M_0}{V_A}$. $i_{AT} = \frac{I_T}{I_A}$, $k_{AT} = \frac{K_T}{K_A}$, $v_{AT} = \frac{V_T}{V_A}$.

It can be seen that the number of parameters in the first of the two dimensionless model equations has decreased from five to two. In the second equation, the number of parameters has not changed. Taking into account the fact that the torsion moment in both equations is the same, the total number of

parameters became equal to six, which is less than the nine parameters of the dimensional model (6)–(7).

We estimated the values of the coefficients of dimensionless model equations (30)–(31) and presented them in Table 3.

Table 3. Values of the coefficients of dimensionless model equations (30)–(31).

Coefficients	Estimated values
i_{AT}	0.64
k_{AT}	0.68
v_{AT}	0.68
$\tilde{\beta}_A$	0.01
$\tilde{\beta}_T$	0.007
$\widetilde{M}_{0,A}$	0.01

Note that, in the case of dimensional equations (4)–(5), it was difficult to judge which coefficients were large and which were small. In the dimensionless case, the difference became obvious. The dimensionless coefficients in equation (29), $\tilde{\beta}_A$ and $\widetilde{M}_{0,A}$, are much less than unity. And, in equation (30), the coefficients $\tilde{\beta}_T$ and $\widetilde{M}_{0,T}$ are less than the coefficients i_{AT}, k_{AT} and v_{AT}. And, this indicates that the effects of dissipation and the impact of the torsion moment are really small. This means that the use of perturbation theory in deriving the McLaughlin-Scott equation is quite reasonable.

3.1. Case $\tilde{\beta}_A = 0$, $\tilde{\beta}_T = 0$ and $\widetilde{M}_{0,A} = 0$

In the particular case when the effects of dissipation and external action are negligibly small equation (30) takes the form of the classical canonical sine-Gordon equation (1), which has no coefficients:

$$\varphi_{A,\tau\tau} - \varphi_{A,\xi\xi} + \sin\varphi_A = 0. \tag{32}$$

At the same time equation (31) retains all three coefficients:

$$i_{AT}\varphi_{T,\tau\tau} - k_{AT}\varphi_{T,\xi\xi} + v_{AT}\sin\varphi_T = 0. \tag{33}$$

Hamiltonians corresponding to equations (32) and (33) have the following form:

$$\widetilde{H}_A = \int \left(\frac{\varphi_{A,\tau}^2}{2} + \frac{\varphi_{A,\xi}^2}{2} + (1 - \cos\varphi_A)\right) d\xi, \tag{34}$$

$$\widetilde{H}_T = \int \left(i_{AT}\frac{\varphi_{T,\tau}^2}{2} + k\frac{\varphi_{T,\xi}^2}{2} + v_{AT}(1 - \cos\varphi_T)\right) d\xi. \tag{35}$$

To obtain one-soliton solutions of equations (32), (33), we take dimensional solutions (11) and (12) and rewrite them with new variables:

$$\tilde{\varphi}_{k,A}(\xi,\tau) = 4\text{arctg}\left\{\exp\left[(\gamma_A)\left(\xi - \frac{v_{k,A}}{C_A}\cdot\tau - \xi_{0,A}\right)\right]\right\}, \tag{36}$$

$$\tilde{\varphi}_{k,T}(\xi,\tau) = 4\text{arctg}\left\{\exp\left[(\gamma_T)\frac{d_A}{d_T}\left(\xi - \frac{v_{k,T}}{C_A}\cdot\tau - \xi_{0,T}\right)\right]\right\}. \tag{37}$$

Substituting the solutions into the Hamiltonians (34), (35) we find the total kink energies:

$$\tilde{E}_A = \tilde{E}_{0A}\,\gamma_A, \tag{38}$$

$$\tilde{E}_T = \tilde{E}_{0T}\,\gamma_T, \tag{39}$$

where $\tilde{E}_{0A}, \tilde{E}_{0T}$ are the kink rest energies:

$$\tilde{E}_{0A} = 8, \tag{40}$$

$$\tilde{E}_{0T} = 8\sqrt{k_{AT}v_{AT}}. \tag{41}$$

3.2. Case $\tilde{\beta}_A \neq 0$, $\tilde{\beta}_T \neq 0$ and $\tilde{M}_{0,A} \neq 0$

In the general case, when $\tilde{\beta}_A \neq 0$, $\tilde{\beta}_T \neq 0$ and $\tilde{M}_{0,A} \neq 0$ the solutions of equations (30) and (31) have the following form:

$$\tilde{\varphi}_{k,A}(\xi,\tau) = 4\text{arctg}\{exp[(\gamma_A)(\xi - \tilde{v}_{k,A}(\tau)\cdot\tau - \xi_{0,A})]\}, \tag{42}$$

$$\tilde{\varphi}_{k,T}(\xi,\tau) = 4\text{arctg}\left\{\exp\left[(\gamma_T)\frac{d_A}{d_T}(\xi - \tilde{v}_{k,T}(\tau)\cdot\tau - \xi_{0,T})\right]\right\}, \tag{43}$$

where $\tilde{v}_{k,A} = \frac{v_{k,A}(\tau)}{C_A}$ and $\tilde{v}_{k,T} = \frac{v_{k,T}(\tau)}{C_A}$ are dimensionless kink velocities which are respectively determined by the following equations:

$$\frac{d}{d\tau}\tilde{v}_{k,A} = -\tilde{\beta}_A\tilde{v}_{k,A}\left(1 - {\tilde{v}_{k,A}}^2\right) + \frac{M_0\pi}{4V_A}\left(1 - {\tilde{v}_{k,A}}^2\right)^{3/2}, \tag{44}$$

$$\frac{d}{d\tau}\tilde{v}_{k,T} = -\tilde{\beta}_T(\tilde{v}_{k,T})\left(1 - {\tilde{v}_{k,T}}^2\left(\frac{C_A}{C_T}\right)^2\right) + \frac{M_0\pi}{4V_A}\frac{1}{\sqrt{i_{AT}v_{AT}}}\left(\frac{C_T}{C_A}\right)\left(1 - {\tilde{v}_{k,T}}^2\left(\frac{C_A}{C_T}\right)^2\right)^{3/2}. \tag{45}$$

Equations (44) and (45) were solved numerically using the parameter values from Table 1. Figure 3a and 3b present the results obtained for the dimensionless kink velocities ($\tilde{v}_{k,A}, \tilde{v}_{k,T}$) and coordinates ($\tilde{\xi}_{k,A}, \tilde{\xi}_{k,T}$). The latter were determined by the following relations:

$$\tilde{v}_{k,A} = \frac{d}{d\tau}\tilde{\xi}_{k,A}, \qquad \tilde{v}_{k,T} = \frac{d}{d\tau}\tilde{\xi}_{k,T}. \tag{46}$$

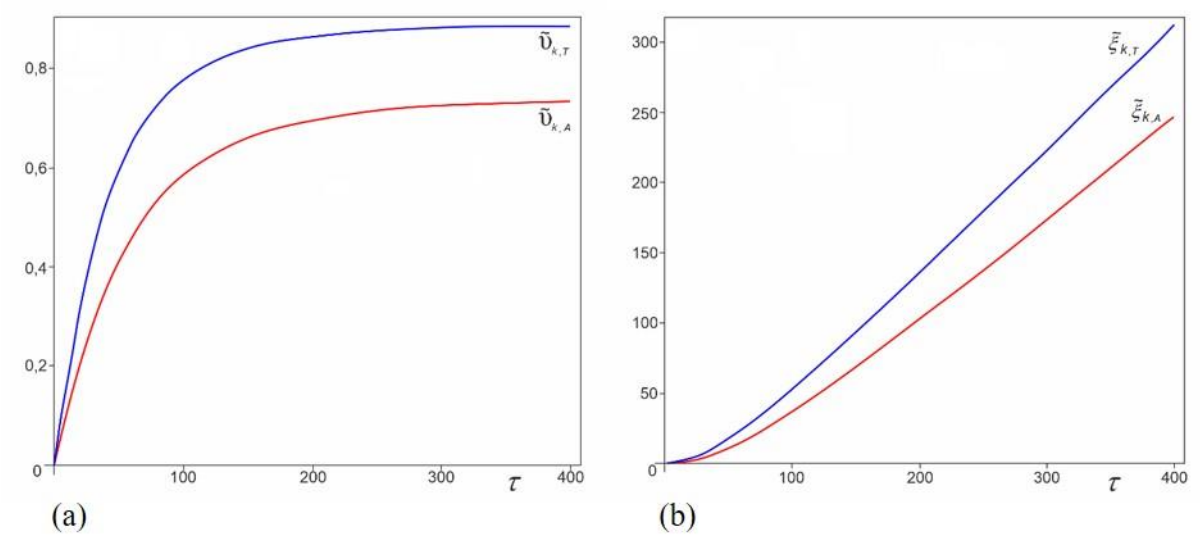

Figure 3. Time dependence of the kink dimensionless velocities (a) and coordinates (b). Red curves refer to the kinks propagating in the poly(A) chain and blue curves refer to the kinks propagating in the poly(T) chain. The calculations were carried out with the help of equations (44)–(46) and the parameters presented in Table 3. The initial kink velocities were suggested to be zero.

Figure 3 shows that as, the time τ increases, the kink velocities and coordinates increase monotonically. As $\tau \to \infty$, the velocities tend to the stationary values $\tilde{v}_{st,A} = 0.68$ and $\tilde{v}_{st,T} = 0.85$, and the coordinates tend to infinity.

4. Discussion and conclusions

In this work, we have constructed the dimensionless analog of the model simulating the dynamics of transcription bubbles and demonstrated the method of constructing in detail. As a basic dimensional model, we used a system of nonlinear differential equations proposed in [16], the one-soliton solutions of which (kinks) were interpreted as mathematical images of transcription bubbles. The main results, including equations of motion, kink-like solutions, kink rest energy, and total kink energy obtained for the dimensionless model, are presented in Table 4.

Table 4. Basic formulas calculated for dimensionless model of homogeneous DNA.

Parameters	Model characteristics	Kink movement in the poly(A) chain	Kink movement in the poly(T) chain
$\tilde{\beta}_A = 0,$ $\tilde{\beta}_T = 0,$ $\tilde{M}_{0,A} = 0$	Equations of motion	$\varphi_{A,\tau\tau} - \varphi_{A,\xi\xi} + \sin\varphi_A = 0$	$i_{AT}\varphi_{T,\tau\tau} - k_{AT}\varphi_{T,\xi\xi} + v_{AT}\sin\varphi_T = 0$
	Hamiltonian	$\tilde{H}_A = \int \left(\frac{\varphi_{A,\tau}^2}{2} + \frac{\varphi_{A,\xi}^2}{2} + (1 - \cos\varphi_A)\right) d\xi,$	$\tilde{H}_T = \int \left(i_{AT}\frac{\varphi_{T,\tau}^2}{2} + k\frac{\varphi_{T,\xi}^2}{2} + v_{AT}(1 - \cos\varphi_T)\right) d\xi$
	Kink-like solution	$\tilde{\varphi}_{k,A}(\xi,\tau) = 4\text{arctg}\{\exp[\gamma_A(\xi - \tilde{v}_{k,A}(\tau)\cdot\tau - \xi_{0,A})]\}$	$\tilde{\varphi}_{k,T}(\xi,\tau) = 4\text{arctg}\{\exp[\gamma_T\left(\frac{d_A}{d_T}\right)(\xi - \tilde{v}_{k,T}(\tau)\cdot\tau - \xi_{0,T}]\}$
	Total energy	$\tilde{E}_A = 8\gamma_A$	$\tilde{E}_T = \tilde{E}_{0T}\,\gamma_T$
	Rest energy	$\tilde{E}_{0A} = 8$	$\tilde{E}_{0T} = 8\sqrt{k_{AT}v_{AT}}$
$\tilde{\beta}_A \neq 0,$ $\tilde{\beta}_T \neq 0,$ $\tilde{M}_{0,A} \neq 0$	Equations of motion	$\varphi_{A,\tau\tau} - \varphi_{A,\xi\xi} + \sin\varphi_A = -\tilde{\beta}_A\varphi_{A,\tau} + \tilde{M}_{0,A}$	$i_{AT}\varphi_{T,\tau\tau} - k_{AT}\varphi_{T,\xi\xi} + v_{AT}\sin\varphi_T = -\tilde{\beta}_T\varphi_{T,\tau} + \tilde{M}_{0,T}$
	Kink-like solution	$\tilde{\varphi}_{k,A}(\xi,\tau) = 4\text{arctg}\{\exp[\gamma_A(\xi - \tilde{v}_{k,A}\cdot\tau - \xi_{0,A})]\}$	$\tilde{\varphi}_{k,T}(\xi,\tau) = 4\text{arctg}\{\exp[\gamma_T\left(\frac{d_A}{d_T}\right)(\xi - \tilde{v}_{k,T})\cdot\tau - \xi_{0,T}]\}$
	Equation for kink velocity	$\frac{d\tilde{v}_{k,A}}{d\tau} = -\tilde{\beta}_A\tilde{v}_{k,A}\left(1 - \tilde{v}_{k,A}{}^2\right) + \frac{M_0\pi}{4V_A}\left(1 - \tilde{v}_{k,A}{}^2\right)^{3/2}$	$\frac{d\tilde{v}_{k,T}}{d\tau} = -\tilde{\beta}_T\left(\tilde{v}_{k,T}\right)\left(1 - \tilde{v}_{k,T}{}^2\left(\frac{C_A}{C_T}\right)^2\right) + \frac{M_0\pi}{4V_A}\frac{1}{\sqrt{i_{AT}v_{AT}}}\left(\frac{C_T}{C_A}\right)\left(1 - \tilde{v}_{k,T}{}^2\left(\frac{C_A}{C_T}\right)^2\right)$

For comparison, we present in Table 5, similar results obtained for the corresponding dimensional model.

Table 5. Basic formulas calculated for dimensional model of homogeneous DNA.

Parameters	Model characteristics	Kink movement in the poly(A) chain	Kink movement in the poly(T) chain
$\beta_A = 0,$ $\beta_T = 0,$ $M_0 = 0$	Equations of motion	$I_A\varphi_{A,tt} - K_A^{/}a^2\varphi_{A,zz}$ $+V_A\sin\varphi_A = 0$	$I_T\varphi_{T,tt} - K_T^{/}a^2\varphi_{T,zz}$ $+V_T\sin\varphi_T = 0$
	Hamiltonian	$H_A = \int (I_A\frac{\varphi_{A,t}^2}{2} + K_A^{/}a^2\frac{\varphi_{A,t}^2}{2}$ $+V_A(1-\cos\varphi_A))\frac{dz}{a}$	$H_T = \int (I_T\frac{\varphi_{T,t}^2}{2} + K_T^{/}a^2\frac{\varphi_{T,t}^2}{2}$ $+V_T(1-\cos\varphi_T))\frac{dz}{a}$
	Kink-like solution	$\varphi_{k,A}(z,t)$ $= 4\text{arctg}\{\exp[(\gamma_A/d_A)(z -$ $-v_{k,A}\cdot t - z_{0.A})]\}$	$\varphi_{k,T}(z,t)$ $= 4\text{arctg}\{\exp[(\gamma_T/d_T)(z -$ $-v_{k,T}\cdot t - z_{0.T})]\}$
	Total energy	$E_A = E_{0,A}\cdot\gamma_A$	$E_T = E_{0,T}\cdot\gamma_T$
	Rest energy	$E_{0,A} = 8\sqrt{K_A'V_\text{A}}$	$E_{0,T} = 8\sqrt{K_T'V_\text{T}}$
$\beta_A \neq 0,$ $\beta_T \neq 0,$ $M_0 \neq 0$	Equations of motion	$I_A\varphi_{A,tt} - K_A^{/}a^2\varphi_{A,zz}$ $+V_A\sin\varphi_A = -\beta_A\varphi_{A,t} + M_0$	$I_T\varphi_{T,tt} - K_T^{/}a^2\varphi_{T,zz}$ $+V_T\sin\varphi_T = -\beta_T\varphi_{T,t} + M_0$
	Kink-like solution	$\varphi_{k,A}(z,t)$ $= 4\text{arctg}\{\exp[(\gamma_A/d_A)(z -$ $-v_{k,A}(t)\cdot t - z_{0.A})]\}$	$\varphi_{k,T}(z,t)$ $= 4\text{arctg}\{\exp[(\gamma_T/d_T)(z -$ $-v_{k,T}(t)\cdot t - z_{0.T})]\}$
	Equation for kink velocity	$\frac{dv_{k,A}^{/}(t)}{dt} =$ $-\frac{\beta_A}{I_A}v_{k,A}^{/}(t)(1-v_{k,A}^{/2}(t))$ $+\frac{M_0\pi}{4\sqrt{I_AV_A}}(1-v_{k,A}^{/2}(t))^{3/2}$	$\frac{dv_{k,T}^{/}(t)}{dt} =$ $-\frac{\beta_T}{I_T}v_{k,T}^{/}(t)(1-v_{k,T}^{/2}(t))$ $+\frac{M_0\pi}{4\sqrt{I_TV_T}}(1-v_{k,T}^{/2}(t))^{3/2}$

It can be seen that the dimensionless model has advantages over the dimensional one. Indeed, carrying out the procedure of transformation of the dimensional model to the dimensionless one leads to the decrease in the number of model parameters from 9 to 6. Moreover, in the framework of the dimensionless analog, it became obvious that the coefficients in the terms simulating the dissipation effects and the action of a constant torsion moment are really small, which proves the validity of the application of the perturbation theory and the method of McLaughlin and Scott.

It should be noted, however, that in order to simplify calculations and to present the procedure of transition to dimensionless form more clear, we limited ourselves to the case of homogeneous (synthetic) DNA. Obviously, the next step in the development of this direction can be the construction of a dimensionless analog for the case of inhomogeneous DNA. This will provide an answer to the question of whether the advantages of the dimensionless model will be preserved in the inhomogeneous case.

One more step could be the improvement if the dimensional model itself by removing the

limitations and simplifications detailed in Section 2. Finally, one could consider the issue of DNA kinks being created by mutual DNA-DNA interactions, which were considered theoretically in [38,39], and experimentally in [40].

Use of AI tools declaration

The authors declare they have not used Artificial Intelligence (AI) tools in the creation of this article.

Conflict of interest

All authors declare no conflicts of interest in this paper.

References

1. Alberts B, Johnson A, Lewis J, et al. (2015) *Molecular Biology of the Cell*. New York: W.W. Norton Company. https://doi.org/10.1201/9781315735368
2. Severin ES (ed.) (2004) Biochemistry, Moscow: GEOTAR–Media. Available from: https://teacher.3dn.ru/Files/bio_med/severin_bioh.pdf
3. Makasheva KA, Endutkin AV, Zharkov DO (2019) Requirements for DNA bubble structure for efficient cleavage by helix-two-turn-helix DNA glycosylases. *Mutagenesis* 35: 119–128. https://doi.org/ 10.1093/mutage/gez047
4. Hillebrand M, Kalosakas G, Bishop AR, et al. (2021) Bubble lifetimes in DNA gene promoters and their mutations affecting transcription. *J Chem Phys* 155: 095101. https://doi.org/10.1063/5.0060335
5. Grinevich AA, Ryasik AA, Yakushevich LV (2015) Trajectories of DNA bubbles. *Chaos, Soliton Fract* 75: 62–75. https://doi.org/10.1016/j.chaos.2015.02.009
6. Shikhovtsova ES, Nazarov VN (2016) Nonlinear longitudinal compression effect on dynamics of the transcription bubble in DNA. *Biophys Chem* 214–215: 47–53. https://doi.org/10.1016/j.bpc.2016.05.005
7. Scott AC, Chu FYF, McLaughlin DW (1973) The soliton: a new concept in applied science. *Proc IEEE* 61: 1443–1483. https://doi: 10.1109/proc.1973.9296
8. Caudrey PJ, Eilbeck JC, Gibbon JD (1975) The sine-Gordon equation as a model classical field theory. *Nuovo Cim B* 25: 497–512. https://doi.org/10.1007/BF02724733
9. Englander SW, Kallenbach NR, Heeger AJ, et al (1980) Nature of the open state in long polynucleotide double helices: possibility of soliton excitations. *Proc Natl Acad Sci USA* 77: 7222–7226. https://doi: 10.1073/pnas.77.12.7222
10. McLaughlin DW, Scott AC (1978) Perturbation analysis of fluxon dynamics. *Phys Rev A* 18: 1652. https://doi.org/10.1103/PhysRevA.18.1652
11. McLaughlin DW, Scott AC (1978) A multisoliton perturbation theory. In: Lonngren, K., Scott, A., *Solitons in Action*, New York: Academic Press. https://doi.org/10.1016/B978-0-12-455580-8.50015-9

12. Zarubin S, Markelov GE (2013) Lectures on the foundations of mathematical modeling. Moscow: State Technical University named after N.E. Bauman. Available from: https://studfile.net/preview/1683378
13. Rasmuson A, Andersson B, Olsson L, et al (2014) *Mathematical Modeling in Chemical Engineering*, New York: United States of America by Cambridge University Press. https://doi.org/10.1002/cite.201590043
14. Torain DS (2014) A dimensionless mathematical model. *Am Rev Math Stat* 2: 01–16. https://doi: 10.15640/arms.v2n2a1
15. Langtangen HP, Pederse GK (2016) Dimensions and units, *Scaling of Differential Equations*, Springer. https://doi.org/10.1007/978-3-319-32726-6_1
16. Grinevich AA, Masulis IS, Yakushevich LV (2021) Mathematical modeling of transcription bubble behavior in the pPF1 plasmid and its modified versions: The link between the plasmid energy profile and the direction of transcription. *Biophysics* 66: 248–258. https://doi:10.1134/s000635092102007x
17. Peyrard M, Bishop AR (1989) Statistical mechanics of a nonlinear model for DNA denaturation. *Phys Rev Lett* 62: 2755–2758. https://doi: 10.1103/physrevlett.62.275
18. Muto V, Scott AC, Christiansen PL (1989) Microwave and thermal generation of solitons in DNA. *J Phys Colloques* 50: 217–222. https://doi: 10.1051/jphyscol:1989333
19. Frank-Kamenetskii MD, Lazurkin YS (1974) Conformational changes in DNA molecules. *Annu Rev Biophys Bioeng* 3: 127–150. https://doi: 10.1146/annurev.bb.03.060174.001015
20. Frank-Kamenetsky MD (1983) *The Most Important Molecule of Life*. Moscow: Nauka.
21. Frank-Kamenetsky MD, Vologodsky AV (1981) Topological aspects of the physics of polymers: The theory and its biophysical applications. *Sov Phys Usp* 24: 679. https://doi:10.1070/pu1981v024n08abeh004835
22. Yakushevich LV, Krasnobaeva LA, Shapovalov AV, et al. (2005) One- and two-soliton solutions of the sine-Gordon equation as applied to DNA. *Biophysics* 50: 450–455.
23. Yakushevich LV, Krasnobaeva LA (2016) Forced oscillations of DNA bases. *Biophysics* 61: 241–250. https://doi.org/10.1134/S000635091602024X
24. Scott AC (1969) A nonlinear Klein-Gordon equation. *Am J Phys* 37: 52–61. https://doi.org/10.1119/1.1975404
25. Taylor JR (1991) Optical Solitons: Theory and Experiment Cambridge. Available from: https://assets.cambridge.org/97805214/05485/toc/9780521405485_toc.pdf
26. Kivshar YS, Malomed BA (1989) Dynamics of solitons in nearly integrable systems. *Rev Mod Phys* 61: 763–915. https://doi.org/10.1103/revmodphys.61.763
27. Braun OM, Kivshar YS (1998) Nonlinear dynamics of the Frenkel-Kontorova model. *Phys Rep* 306: 1–108. https://doi.org/10.1016/S0370-1573(98)00029-5
28. Kulik IO (1967) Wave propagation in a Josephson tunnel junction in the presence of vortices and the electrodynamics of weak superconductivity. *JETP* 24: 1307-1317. Available from: http://jetp.ras.ru/cgi-bin/dn/e_024_06_1307.pdf
29. Malomed BA (1988) Interaction of a soliton with an impurity in the sine-Gordon model of a commensurate charge-density-wave system. *J Phys C Solid State Phys* 21: 5163–5181. http:// doi:10.1088/0022-3719/21/29/013
30. Frenkel YI, Kontorova T (1939) On the theory of plastic deformation and twinning. *Acad Sci USSR J Phys* 1: 137–149.

31. Gerus AI, Vikulin AV (2016) Rotational model of a block geoenvironment: mathematical aspects and numerical results. In: Materials of the regional scientific conference “Volcanism and related processes” dedicated to the Volcanologist's IViS FEB RAS, Petropavlovsk-Kamchatsky, 116– 121.
32. Zharnitsky V, Mitkov I, Levi M (1998) Parametrically forced sine-Gordon equation and domain wall dynamics in ferromagnets. *Phys Rev B* 57: 5033–5035. https://doi.org/10.1103/PhysRevB.57.5033
33. Zharnitsky V, Mitkov I, Gronbech-Jensen N (1998) π kinks in strongly ac driven sine-Gordon systems. *Phys Rev E* 58: 52–55. https://doi.org/10.48550/arXiv.patt-sol/9809011
34. Scott AC (1985) Biological Solitons in: Dynamical Problems in Soliton Systems Springer: Berlin, Heidelberg P. 224–235. https://doi.org/10.1007/978-3-662-02449-2_33
35. Yakushevich LV (2004) Nonlinear physics of DNA, Weinheim: Wiley. Available from: http://ndl.ethernet.edu.et/bitstream/123456789/12866/1/Ludmila%20V.%20Yakushevich_.pdf
36. Dauxois T, Peyrard M (2006) Physics of Solitons. Cambridge: Cambridge University Press. Available from: ttps://assets.cambridge.org/97805218/54214/frontmatter/9780521854214_frontmatter.pdf
37. Yakushevich LV, Krasnobaeva LA (2021) Ideas and methods of nonlinear mathematics and theoretical physics in DNA science: the McLaughlin-Scott equation and its application to study the DNA open state dynamics. *Biophys Rev* 13: 315–338. https://doi.org/10.1007/s12551-021-00801-0
38. Kornyshev AA, Wynveen A (2004) Nonlinear effects in the torsional adjustment of interacting DNA. *Phys Rev E* 69: 041905. https://doi.org/10.1103/PhysRevE.69.041905
39. Cherstvy AG, Kornyshev AA (2005) DNA melting in aggregates: impeded or facilitated? *J Phys Chem B* 109: 13024–13029. https://doi.org/10.1021/jp051117i
40. Sebastiani F, Pietrini A, Longo M, et al. *(*2014) Melting of DNA nonoriented fibers: a wide-angle X-ray diffraction study. *J Phys Chem B* 118: 3785–3792. https://doi.org/10.1021/jp411096d

AIMS Press